

Combination of Planar Laser Optical Measurement Techniques for the Investigation of Pre-mixed Lean Combustion

Lena Lange*, Johannes Heinze, Michael Schroll,
Christian Willert, Thomas Behrendt

Institute of Propulsion Technology, German Aerospace Center (DLR), 51147 Cologne, Germany

*correspondent author: lena.lange@dlr.de

Abstract This paper summarizes recent efforts of applying combinatory or simultaneous multifaceted planar laser optical measurement techniques in reactive flow. The homogeneous (partially) premixed lean combustion in aircraft engines is the most promising combustion concept for the sustainable reduction of fuel consumption and emissions. The concept requires a 30 - 40 % reduction in cooling air flow. These changes require an efficient cooling concept to deal with the increased demands like higher cooling air temperature, higher pressure and reduced cooling air flow. Overall the demands on the homogeneity of the temperature distribution in the reactive flow increase to take into account the increased heat load on the walls at lean combustion. Planar optical measurement techniques capable of providing different measurands were successfully combined in a common set up to enable rapid data acquisition consecutively or even simultaneously. Within a high pressure single sector combustor (SSC) the interaction between a pre-mixed lean flame and the near wall cooling film is observed at realistic pressure (here 5 bars) and preheat temperature (450 K). One of the main advantages of the SSC facility is its optical accessibility from three sides. In the present application an effusion-cooled wall with a mesh of cooling air holes represents the fourth side in the SSC and serves for the qualification of the laser optical measurement techniques for near wall investigations. A first assessment of the combustor design is achieved by the acquisition of the global velocity field, the spatial release of heat, the temperature field and the pre-mixing behavior of the cooling air concept within a central (symmetry) plane. For this purpose previously established spectroscopic measurement techniques are used such as the chemiluminescence of OH radical for the qualitative visualization of the heat release, the planar laser-induced fluorescence (PLIF) of the OH radical to study the mixing properties of combustor flow and film cooling as well as planar temperature distributions. Particle image velocimetry (PIV) visualized and quantified the swirling, recirculating flow field. The PIV measurements were acquired synchronized with the OH PLIF measurements on a single-pulse basis to obtain correlated information of the velocity field and the [OH] distribution with high spatial and temporal resolution. After global characterization of the combustion flow field near-wall PIV/ LIF measurements were carried out with spatial high resolution in close proximity of the effusion cooled wall in an effort to visualize the structure of the cooling air jets in detail.

1. Introduction

Designers of modern aero engine combustors are facing a large number of design targets to ensure the required performance, emissions, operability, efficiency, costs, reliability and lifetime of the combustor. Among those the fuel efficiency and the emissions of the combustor and thus of the engine are especially relevant for this contribution. The fuel efficiency of an aero engine can be improved by increasing the overall temperature and pressure level which leads to a higher thermodynamic efficiency. With conventional combustor technology, which can be found in almost any present gas turbine aero engine, this approach also leads to increased emissions of nitric oxides (NO_x). The NO_x production rates are highest in near stoichiometric regions which are an inherent feature of conventional combustors. Those regions are created when air jets are mixing with the fuel rich mixture injected by the burners. Here the highest temperatures occur and in combination with the presence of oxygen strongly promote the NO_x formation (see e.g. [9]). As the emission limits for NO_x and also for carbon monoxide (CO) and unburned hydrocarbons (UHC) are becoming increasingly restrictive, engine and combustor development is facing a design conflict regarding the

aspects emissions and fuel efficiency, which can hardly be surpassed in the long term with conventional combustor technology.

The lean combustion concept is considered the most promising approach to achieve an engine which is both more fuel efficient and at the same time has low emissions. Here the air fuel mixture injected by the burners is already lean and in conjunction with partially pre-mixing the existence of near stoichiometric regions can be reduced significantly. By this means the *peak* temperature and thus the NO_x production rate is substantially reduced allowing a further increase of the *overall* temperature level to improve the fuel efficiency. In comparison to conventional combustors a complete redistribution of the air flow into the combustor is required which also affects the amount of air available for cooling of the combustor walls. For a combustor with lean burning primary zone the cooling air consumption has to be reduced by roughly 50% leading to a sparse wall cooling film. Combustor cooling becomes even more demanding as the overall temperature (including cooling air temperature) and pressure level will increase. This requires not only the development of cooling concepts with increased efficiency (see e.g. [3]). The key for the understanding of lean combustion in aero engines is the characterization and understanding of the interaction between the highly turbulent, swirling and reacting burner flow field with the wall cooling film. To the knowledge of the authors, aside from experiments performed at the laboratory scale [18][7][13], there is very little experimental data obtained at realistic operating conditions using non-intrusive laser-optical diagnostic methods.

In order to characterize the interaction between burner flow field and cooling film the measurements are conducted in a single sector combustor with a square cross section, which is operated at elevated pressures; for a description of the test rig see [2][10]. The combustor is equipped with a generic burner fueled with natural gas. The primary zone of the combustor provides optical access from three sides. The fourth side is equipped with an effusion cooled wall which is cooled with preheated air. With this approach the interaction between burner flow field and cooling film can be analyzed in an environment which is characteristic for aero engine combustors operating at realistic test conditions. The present work describes recent efforts in applying both particle image velocimetry (PIV) and planar laser induced fluorescence (PLIF), ideally simultaneously, for the investigation of flame-wall interactions. In the case of PLIF the fluorescence of the OH radical is excited with an UV laser and, with proper calibration, yields quantitative OH concentration data [8]. Simultaneous PIV and PLIF measurements obtained in model combustors are described in literature [12][5], but the present kind of measurements in the vicinity of a cooled wall at elevated pressure are believed to be unique.

2. Materials and Methods

For the experimental investigation of wall-flame interactions a swirl burner was specifically designed such that its flame burns in close proximity to an effusion cooled liner wall. The effusion cooling is provided by a regular array of holes (Figure 1). Both the liner wall and burner are mounted inside a pressurized single sector combustor (SSC) which is designed for the optical investigation of aero-engine combustors operating at realistic (flight relevant) conditions (Figure 2). Measurements of the natural gas fueled combustion were performed at a pressure of 5 bar (0.5 MPa) and an air preheating temperature of 450 K. Natural gas was chosen as fuel to exclude additional issues relating to spray combustion.

The SSC facility has unobstructed optical access to the primary combustion zone from three sides, each using a combination of cooled pressure window and thin combustor liner window. The effusion cooled liner wall comprises the fourth side of the square combustor cross section (102 x 102 mm²). A cooling film of preheated air protects the inside of the liner windows from thermal loading by the flame. The downstream end of the 296 mm long combustor is closed off with a critical nozzle with which the operating pressure is controlled. During operation the complete combustion facility is traversable in three orthogonal directions allowing precise positioning of the

optical diagnostics.

The burner itself is a partially pre-mixed swirl nozzle with a wall-flush, annular exit whose aerodynamics cause the lean flame ($\lambda = 1.2$) to burn in immediate proximity of the liner wall (c.f. Fig 5). This flame structure also results in increased thermal loading of the glass liner windows which causes their optical quality to deteriorate rather quickly and limits the available measurement time. Below the flame impingement area optical measurements are possible for longer durations.

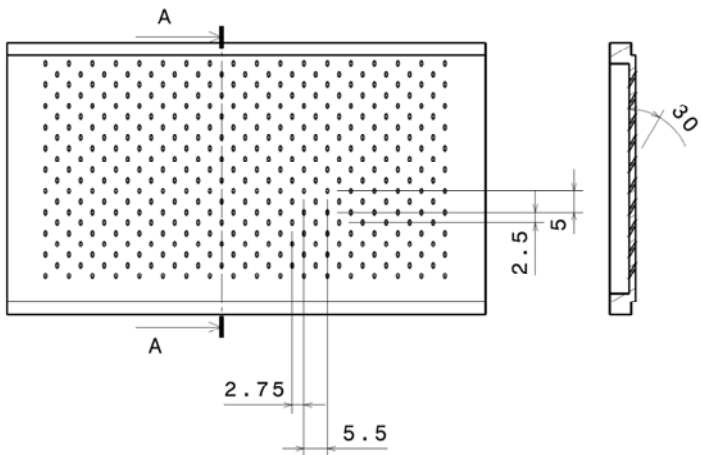


Figure 1: Hole pattern of the effusion cooled liner wall with 0.6 mm diameter holes

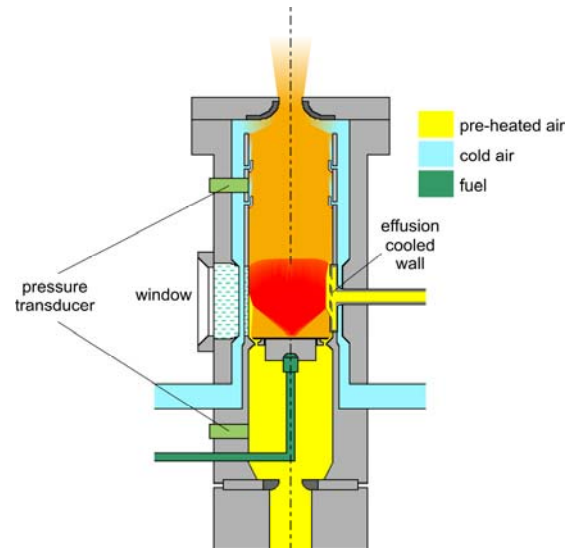


Figure 2: Schematic of the pressurized single-sector combustor (SSC)

For the characterization of the flame wall interaction two laser-optical measurement techniques are combined: PIV for capturing the unsteady flow field and PLIF to provide the matching spatial distribution of the OH concentration. The latter is spectroscopic method which relies on the excitation of the OH radical using UV light of 283 nm. With increasing temperatures the OH concentration exhibits a nearly exponential growth; in lean combustion ($\lambda > 1.1$) this growth is also nearly independent of the air-fuel ratio λ [11]. This feature can be used to infer the instantaneous temperature distribution of lean flames as described in [8]. The exponential growth of the OH concentration results in high temperature sensitivity but at the same time has a lower bound around 1400K below which the presence of OH decreases below the detection threshold.

Figure 3 provides an overview of the measurement setup used for combined PIV and PLIF measurements parallel to the cooled wall. The combined beam of a pulsed UV-laser (283 nm) and a double-pulse PIV-laser (532 nm) is formed into a parallel light sheet and introduced into the combustion chamber. The region of interest within the combustor is observed simultaneously by two cameras via a beam splitter; camera No.1 acquires PIV images while camera No.2 captures the OH-PLIF signal. The beam splitter is designed to reflect light at a wavelength range of 315 ± 10 nm where OH radicals have their primary fluorescence. The chosen measurement setup and triggering scheme ensured that both PIV and PLIF can be applied simultaneously: the two images comprising a single PIV recording straddle each PLIF recording.

The seeding material necessary for PIV consists of porous silica spheres (SiO_2 , 0.5-1.5 μm size range) which is first dispersed using a fluidized bed seeding device [17] and then introduced into the facility at two different positions: the plenum upstream of the combustor as well as the cooling air supplying the effusion cooled liner wall. The latter is used to visualize the cooling air issuing from the effusion cooled wall. Both supply lines can be individually controlled which permits the seeding to be introduced only during the measurement which in turn prevents unnecessary deposition of seeding material on the windows.

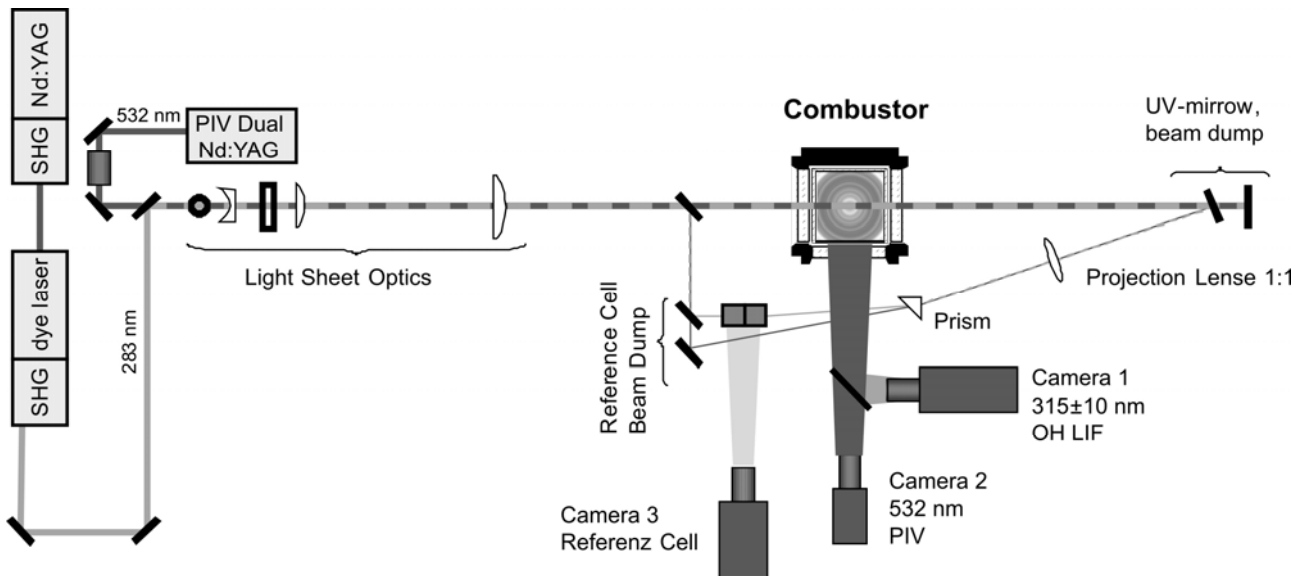


Figure 3: Setup for combined PIV-PLIF measurements parallel to the effusion cooled wall

In the optical arrangement shown in Figure 3 the light sheet can exit the test section on the opposite side which allows absorption correction to be applied to the PLIF signal. This is achieved by the simultaneous measurement of the light intensity profiles before and after passage through the test section using a pair of reference cells [8]. In practice about 1% of the incident laser light sheet is diverted to a quartz glass cuvette filled with an ethanol solution of Rhodamine 6G. In a similar manner the exiting light sheet is imaged into the second reference cell. Dispersion prisms and dichroic mirrors are used to remove the green light of the PIV laser before the remaining UV light enters the reference cells. The position of the reference cells is chosen to match that of the actual measurement area (i.e. combustor) allowing a side-by-side comparison of the intensity profile. The fluorescence within the dye cells is imaged with intensified camera No. 3 in Figure 3 and used to correct the OH fluorescence signal acquired with intensified camera No.1.

While OH-PLIF measurements to within 0.5 mm of the wall are feasible using the wall parallel arrangement of Figure 3, similar PIV measurements were not possible because of strong laser flare on the metal surface in the background. This stray light leads to a strong reduction of signal-to-noise ratio and causes self-correlation on the stationary specular background. The alternative arrangement, shown in Figure 4, is to align the laser light sheet normal to the liner wall to resolve a cross-section of the wall boundary layer. The consequence of this setup is that the light sheet no longer exits the combustor and hence prevents the previously mentioned absorption correction of the OH-PLIF signal. In order to reduce laser flare from the wall to a minimum the optical axis of the PIV camera lens is aligned with liner wall, such that the imaged liner wall is located in the middle of the PIV image.

In absence of possible absorption correction it was decided to use the OH excitation line ($OH\ A-X\ (v'=1, v''=0)\ R_2(8.5)+Q_1(11.5)$), which exhibits about one third the absorption sensitivity as the previously used line ($OH\ A-X\ (v'=1, v''=0)\ Q_1(9.5)+Q_2(7.5)$) [15]. This allows a reduction of the mean uncorrelated absorption within the field of view to about 10% and can be ignored. The choice of this weaker absorption line also cuts the signal strength by about 50% which in the present case was not detrimental. The calibration of the OH signals acquired in the wall normal planes is achieved using the previously calibrated wall-parallel OH concentration measurements. This is possible because the inner recirculation zone exhibits a spatially and temporally stable OH concentration.

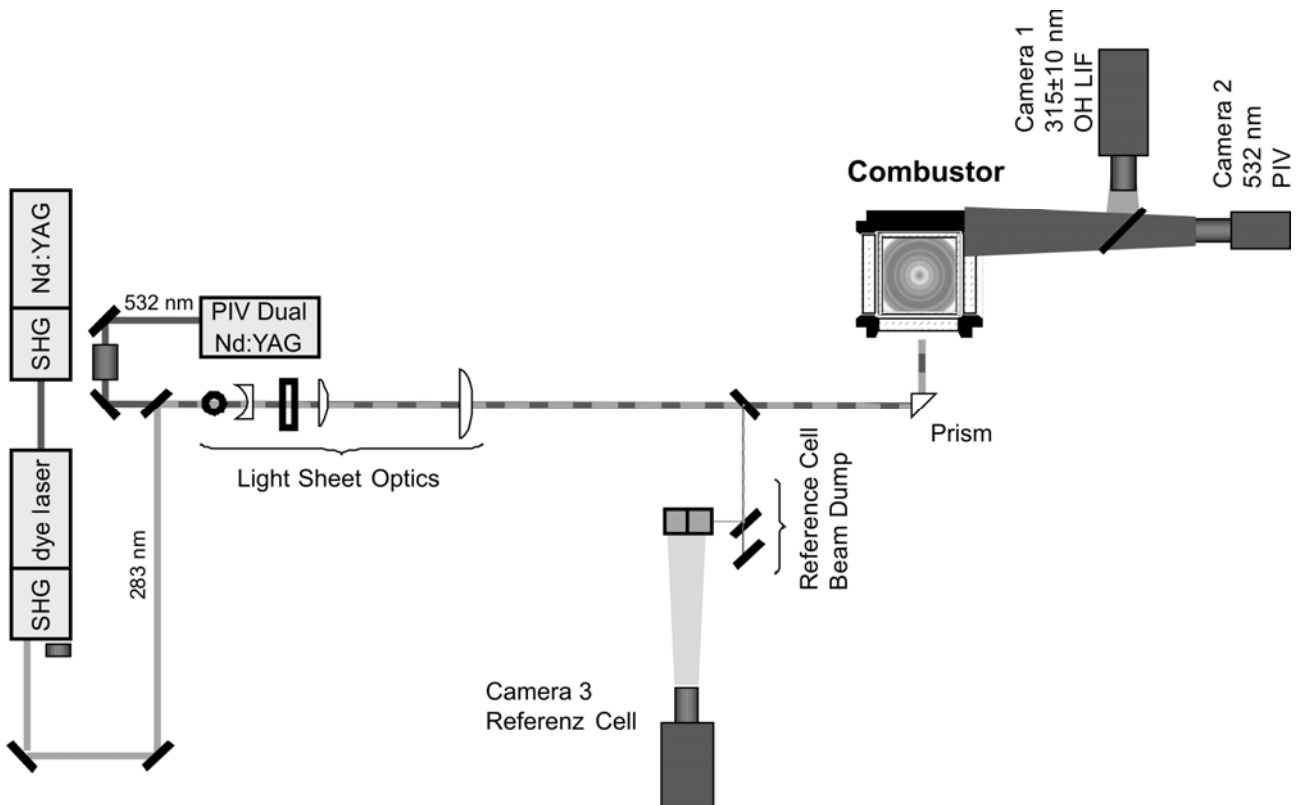


Figure 4: Setup for combined PIV-PLIF measurements normal to the effusion cooled wall

2.1 Experimental Hardware

The OH radical is excited with a narrowband, frequency-doubled dye laser (*LAS, LDL205*) which is pumped by a frequency-doubled Nd:YAG pulse laser (*Spectra Physics, GCR 190-10*). The pulse energy at 283 nm is about 5-10 mJ and 10 Hz repetition rate. The light sheet optics form a light sheet of 48mm height and 0.2 mm waist thickness within the field of view. The emitted OH fluorescence is first spectrally filtered using a combination of interference filter (*Laser Components, 312 ± 15 nm, T > 80%*) and UV glass filter (*Schott, UG11*) and then imaged with an UV-objective lens (*Cerco, 100mm/F=2.8*) onto a S20 photocathode of an intensified camera (*Kamera 1, PCO Dicam Pro*). For global flow/flame characterization the spatial resolution is 0.18 mm/pixel which correspond to the light sheet thickness. In order to resolve the wall interaction of the combustion the spatial resolution is improved to 0.08 mm/pixel.

The PIV light source consists of a dual cavity, frequency-double Nd:YAG laser with 120 mJ per pulse at 532 nm (*Quantel, Twins BSL140 CFR200*). The light scattered by the silica seeding particles is imaged with a 105 mm/f#2.8 objective lens (*Nikon, Micro-Nikkor 105/2.8*) onto a 2048 x 2048 pixel CCD array with a pixel pitch of 7.4 μm. The CCD camera (*PCO, pco.2000*) is operated in double frame mode to acquire two separate particle image recordings within a few microseconds. When applying PIV image sampling of 32 x 32 pixel the spatial resolution of the recovered velocity field is about 0.39 x 0.39 mm² for the global view and 0.13 x 0.13 mm² is the high magnification mode of operation.

3. Results

To characterise the global velocity and OH field in the centre section of the burner 100 individual images were acquired. In Figure 5 the OH distributions are presented as false color and overlaid with vectors representing the velocity field. Because a particular minimum resolution was necessary in order to be able to resolve the velocities with PIV, only half of the flame is measured, as indicated at the right part of Figure 5

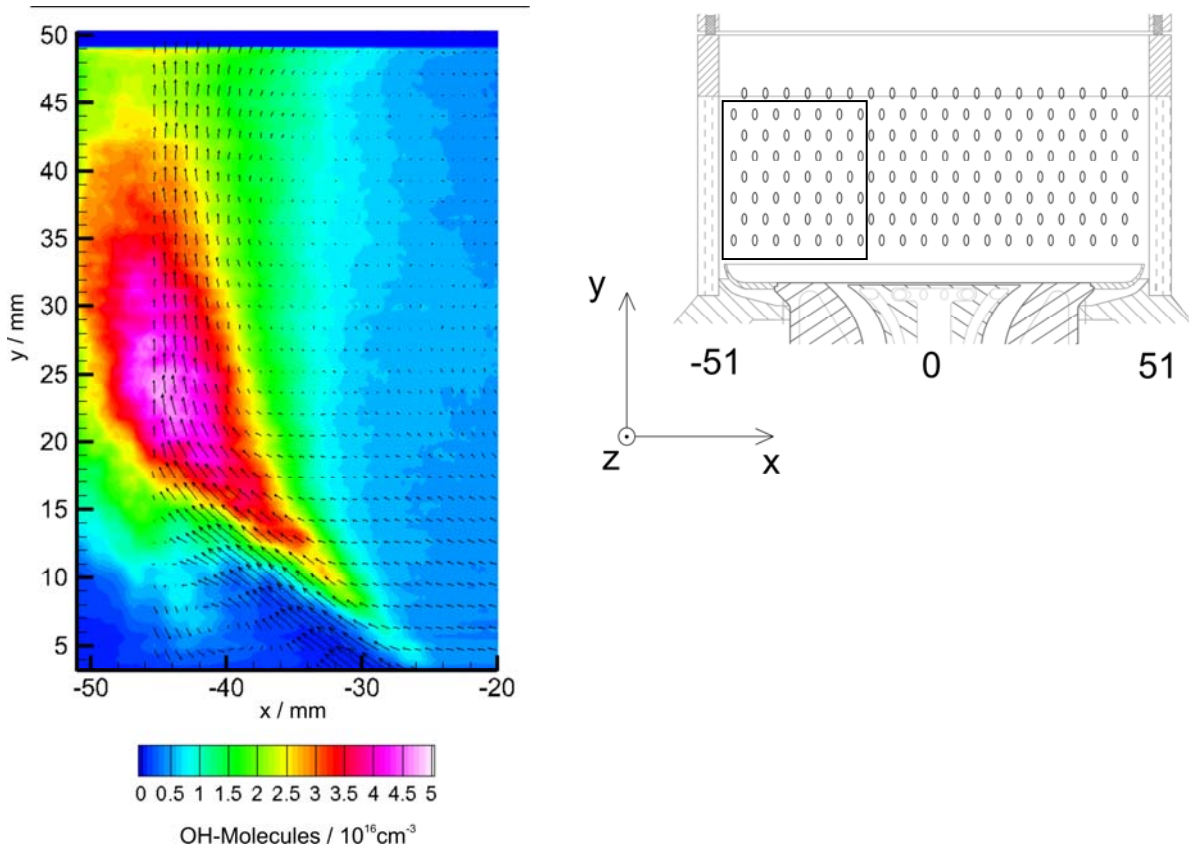


Figure 5: Combined measurement of PIV and PLIF obtained at the mid-plane within the combustor. Pseudo-colors illustrate OH concentration while vectors indicate the underlying flow field. The glass wall is located at $x = -51$ mm

In Figure 5 the hot exhaust gas from the flame is visible as areas of high OH concentration, shown in false colour. It impacts the combustion chamber pane at the left side at a height of 25-30 mm. At the burner outlet, at a radial distance of 30 mm, the highest speeds reach about 50 m/s. In order to measure these high velocities, a pulse separation of approximately $2 \mu\text{s}$ in between the two PIV laser pulses is necessary. The inner recirculation on the right side was not adequately resolved, because it is too slow for the chosen pulse interval. The outer recirculation zone is clearly visible in the lower left part of the velocity field at a radial distance of about 40 mm.

To obtain simultaneous PIV and LIF measurements some compromises were necessary which did not introduce significant disadvantages. On the one hand the addition of seeding into the burner air and the cooling air of the wall was found not to negatively affect the quality of the LIF spectra. On the other hand the astigmatism [4] introduced in the PIV images due to the insertion of an UV beam splitter plate in front of the PIV camera was small enough not to have negative influence on PIV data processing. In essence this enabled the acquisition and subsequent evaluation of the simultaneously recorded PIV and LIF images on a pulse-by-pulse basis. This is illustrated in Figure 6 (left) in which the single pulse of the velocity field is shown in combination with the OH distribution as a heat indicator.

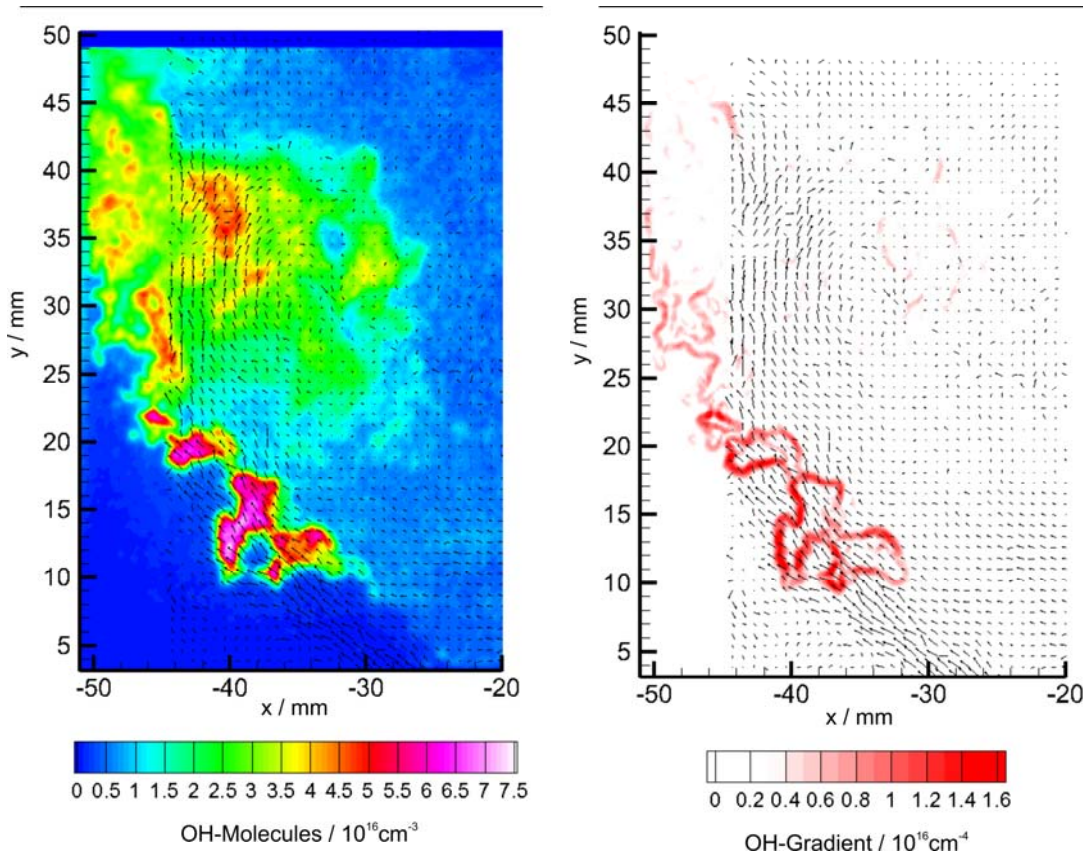


Figure 6: Simultaneous single shot measurement of PIV and OH-PLIF at the combustor mid-plane with colors indicating absolute OH concentration (left) and spatial gradient of OH (right). Vectors indicate underlying flow field.

The flame front is associated with a sharp rise in OH concentration [1][8]. Such a rise can be clearly seen through the gradient of OH concentration to image the spatially and temporally resolved flame front [12][14]. Figure 6 (right) shows the gradient of the OH distribution combined with the velocity field in a snapshot. Here is the relation between the flame front and the velocity field significantly and allows further interpretations of the turbulence-chemistry interaction in flames.

In Figure 6 it can be seen that the hot exhaust gases of the flame (high OH concentration) directly impinges on the wall (in this case the glass liner window). The cooling film of the wall formed mainly from the bottom of the wall and is barely detectable in the range ($y > 20$ mm) of the flame-wall interaction. This proximity of the combustion to the wall leads to a significant reduction of the lifetime of the windows. Within a few minutes the surface of the glowing windows roughens reducing the overall transparency of the window. In combination with the window contamination by the required solid tracer particles the useful measurement time is limited to less than 15 minutes.

With a light sheet placed parallel to the wall measurements are only feasible with PLIF while the PIV technique suffers a loss of signal to noise ratio due to strong reflections on the wall in the background of the scene. As a consequence only multiple PLIF wall parallel planes were measured by traversing through multiple planes in increasing intervals from the wall (Figure 7).

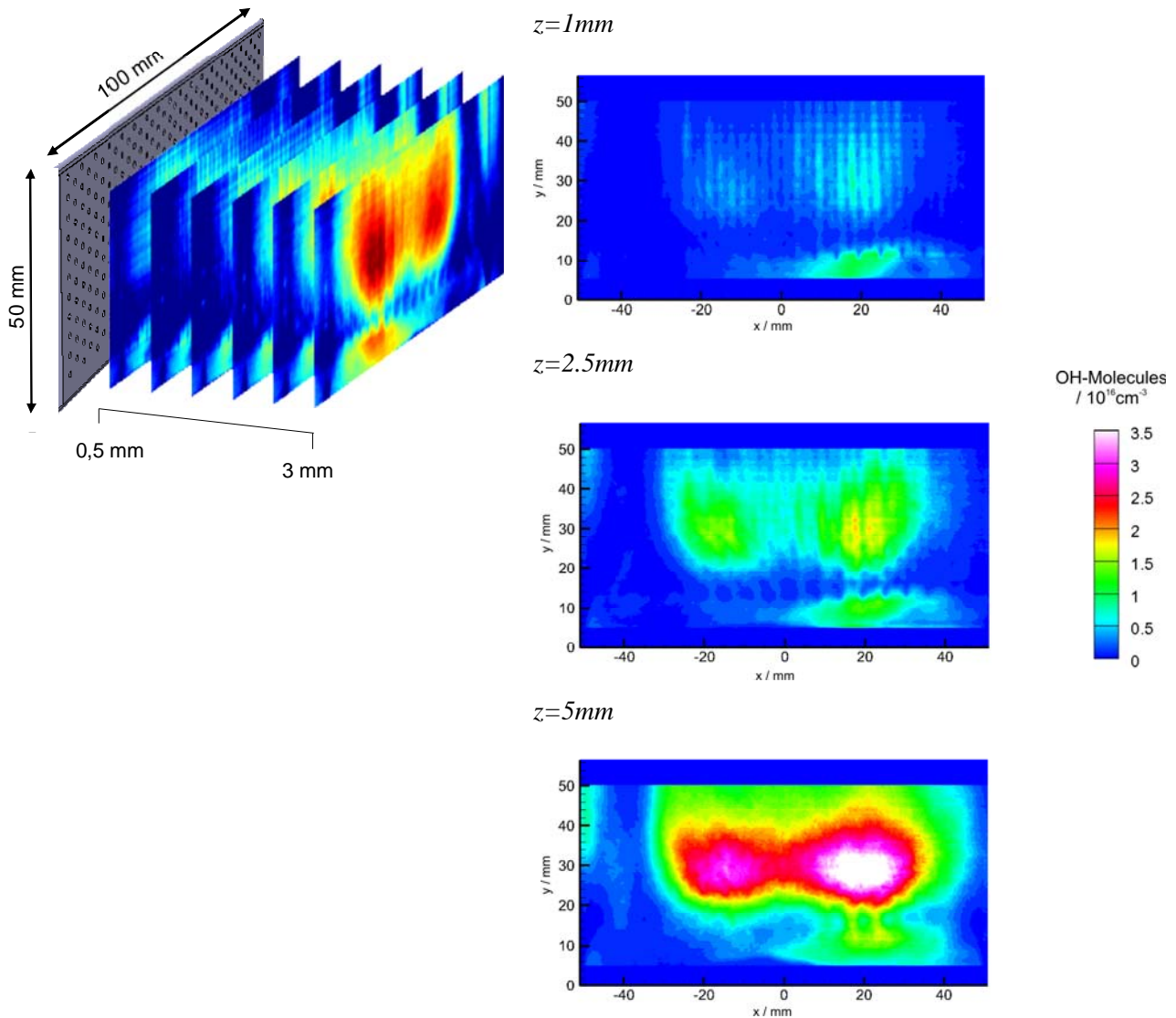


Figure 7: Wall parallel measurements of the OH-concentration obtained at different wall distances z

Figure 7 shows selected OH-concentration planes as examples and indicate that the cooling air jets reach a wall-normal distance of about 1 mm. At greater wall distances the cooling air forms an unstructured cooling film on the wall. The measurements at the smallest wall distance of 0.5 mm from the wall are characterized by strong beam disturbances in the light sheet, resulting from the high refractive index gradients across the high number of cooling jets.

The mean OH concentrations presented in Figure 7 should be interpreted keeping in mind that these are averages of highly unsteady data where, hot flamelets carrying significant OH signal alternate with cooler air packets without any OH signal whatsoever. Closer inspection of the single pulse measurements reveals that the flame does in fact occasionally touch the effusion cooled wall even if the average suggests differently. This means that the effusion film layer is momentarily disrupted.

Because the PIV measurements in the wall-parallel setup were not feasible, a second set of measurements were acquired with the light sheet plane perpendicular to the wall. Figure 8 shows the velocity distribution obtained by PIV in the region below the flame wall interaction.

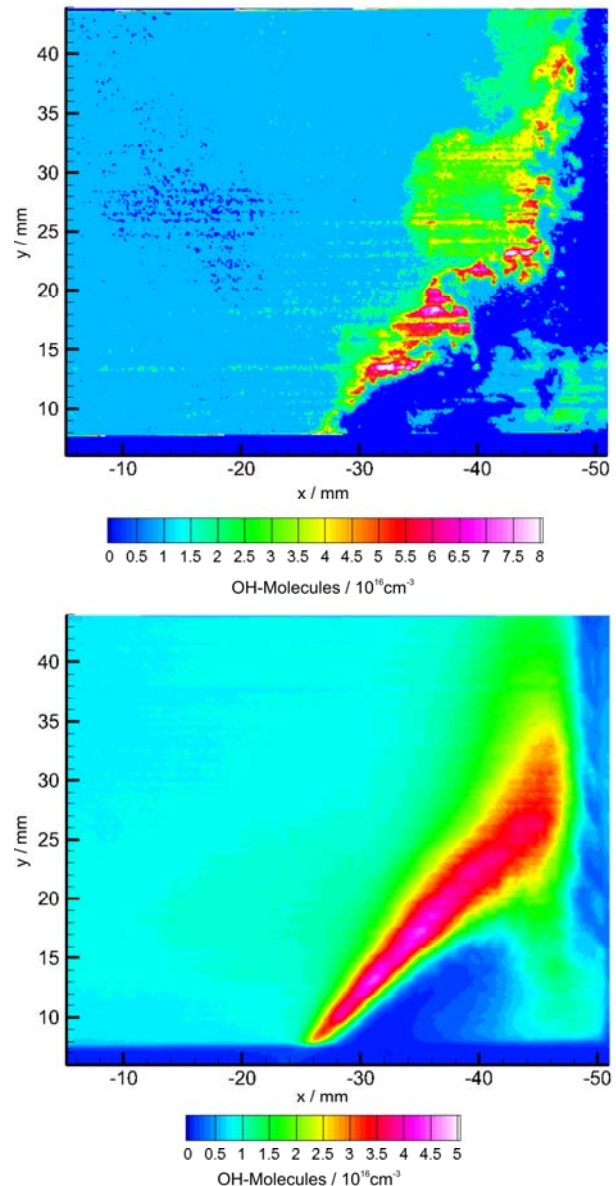
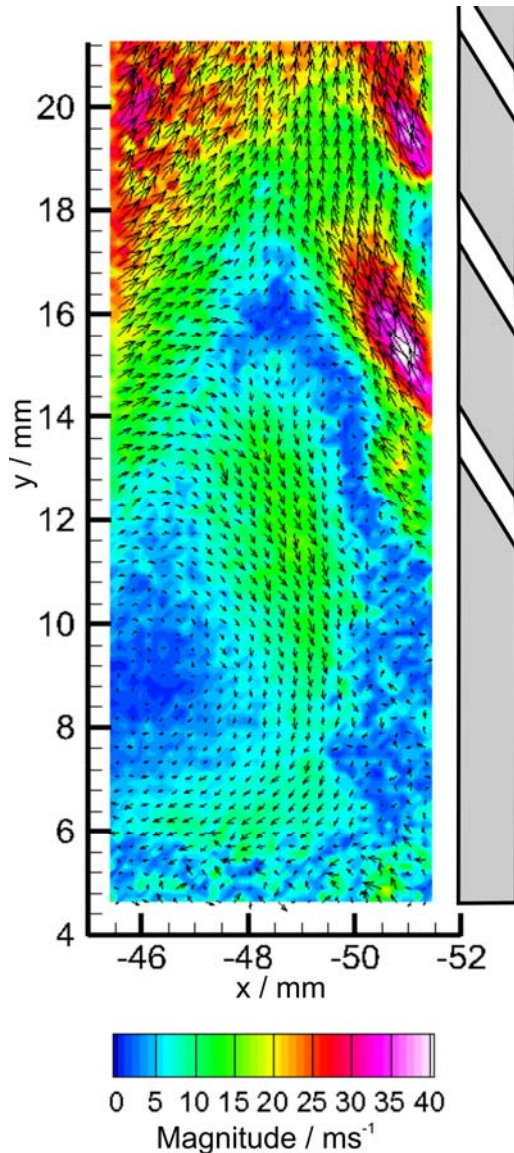


Figure 8: Averaged velocity field near the effusion cooled wall

Figure 9: Near wall measurement of the OH-concentration: single shot result (top) and average of $N = 100$ recordings (bottom)

The evaluation of the PIV measurements in the vertical setup with shifted optical axis could only be evaluated down to a wall distance of greater than 1 mm. This is because the back reflection of the laser light sheet introduced laser flare in the images leading to sensor saturation. Close to the wall thermal and with it density gradients are strongest leading to severe optical distortions including beam steering and internal reflection. As a consequence individual particle images are poorly resolved in this area which manifests itself in low PIV vector validation rates. In essence only a mean velocity map provides useful velocity data (Figure 8). Further downstream along the wall no cooling air jets can actually be resolved. This is in agreement with the results of the PLIF measurements which indicated a cooling jet penetration depth of about 1 mm while the PIV data is limited to wall distances greater than 1 mm.

PLIF measurements with a wall normal light sheet orientation were also carried out. This could be evaluated in single pulse (Figure 9, top). The light sheet distortion due to strong refractive index

gradients induced by the flame is clearly visible in the single pulse images (visible as stripes in Figure 9, top). Although the UV light sheet strikes the metallic wall and generates a lot of scattered light, the reflection is not captured in the pictures, because it is completely suppressed by the spectral filtering of the fluorescence. Nonetheless this scattered light can excite OH LIF from areas outside of the light sheet. This “false” LIF signal provides a diffuse background and limits the lower detection limit of OH close to the wall. While the sensible evaluable dynamic range in the entrance area much larger than 100 (s. Figure 6), it is reduced to less than 50 in close proximity with the wall. Regardless, very fine structures (< 1 mm) can be recognizable. The flame does not directly impinge on the wall as in the case of the film-cooled pane in Figure 5 and Figure 6, but approaches only about 1-2 mm of the wall. This is attributed to the presence of a functioning cooling film along the illustrated light sheet plane aligned with a given vertical column of cooling air holes. While not presented here this film also extends into the areas in between the effusion cooling holes. The cooling air jets themselves are not or only very weakly discernible in the single pulse OH LIF images (s. Figure 9, top).

The presence of cooling air jets becomes visible as characteristic cold regions in the average OH LIF image shown in Figure 9 (bottom). This suggests the effect described above where the flame strikes intermittently impinges on the wall in between the cooling air jets but is deflected by the jets. This behaviour can also be observed in the OH images obtained with the wall parallel light sheet arrangement (Figure 7). There distinctly separated cooling air jets at a wall distance of 1 mm are visible along with vertical lines of the cold structures along each vertical column of cooling air holes (s. Figure 7, top). These structures of the cooling air are significantly reduced at a wall distance of 2.5 mm (s. Figure 7, middle); at a distance of 5 mm the presence of cooling air structures is no longer detectable (s. Figure 7, bottom). Not shown in this context are the results of the wall-normal planes of light in between two vertical columns of holes. This data shows a cooling film of a thickness of about 1 mm in the form of significantly reduced OH concentration indicating the presence of an established cooling film in this area as well. Structures of the neighbouring cooling jets are not directly visible which corresponds to the results of the wall-parallel light sheets (c.f. Figure 7).

4. Discussion and Summarizing Remarks

The aim of the present investigation was to further improve the understanding of the interaction of the flame with an effusion cooled wall at aero-engine relevant operating conditions. Here the combination of PIV and OH-PLIF was chosen to provide simultaneous access to the unsteady flow field and OH concentration, respectively. From a diagnostic point of view the feasibility of such combinatory measurements was successfully demonstrated. In particular the data generated by the global combustor characterization could be processed in its entirety. Close-up views of the reacting flow revealed small scale structures such as the small air jets issuing from 0.6 mm diameter holes in the effusion cooled liner wall. Due to the rather low susceptibility of OH-PLIF to laser flare the technique is suited for both wall-parallel and wall-normal light sheet arrangements. At wall distances of less than 2 mm the reflection of the emitted OH light by the wall reduces the reliability of the OH concentration estimates.

Strong background signal intensities arising from laser flare of a light sheet placed parallel to the wall prevent reliable wall-parallel flow field measurements using PIV. In a wall normal light sheet arrangement this laser flare can be sufficiently suppressed. However in this arrangement the presence of the cooling film and associated high density gradients (and their corresponding turbulent fluctuations) introduce significant optical distortions (e.g. schlieren, beam steering, etc.) that are a hindrance to both measurement techniques. For PIV this results in significant blurring of particle images and complete loss of signal.

Current efforts are directed at improving the PIV technique in order to resolve the flow within 1 mm of the wall and may involve a redesign of the cooling wall in order to reduce the distortions along the optical path between the region of interest and camera.

The near wall measurements presented herein are augmented by density and temperature field measurements obtained with filtered Rayleigh scattering [6]. Capable of resolving the cooling air jets at wall distances in the sub-millimeter range these measurements would benefit from complementary near-wall velocity data obtained by PIV.

Acknowledgements

The authors gratefully acknowledge their colleagues at the Institute for Propulsion Technology, Martin Mueller, Marc Kunter, André Moegelin, and Tobias Conzen for supporting the test campaigns as well as for operating and maintaining the test rig. Thanks go to Melanie Voges and Ulrich Meier for fruitful discussion.

List of References

- [1] Barlow, R.S., Dibble, R.W., Chen, J.-R., Lucht, R.P. (1990): Effect of Damköhler number on superequilibrium OH concentration in turbulent nonpremixed jet flames, *Combust. Flame* 82, pp. 235-251
- [2] Behrendt, T., Frodermann, M., Hassa, Ch., Heinze, J., Lehmann, B., Stursberg, K. (1999): Optical measurements of spray combustion in a single sector combustor from a practical fuel injector at higher pressures, RTO-MP-14, AC/323(AVT)TP/10, pp. 43-1 – 43-12, ISBN 92-837-0009-0
- [3] Behrendt, T., Lengyel, T., Hassa, Ch., Gerendas, M. (2008): Characterization of advanced combustor cooling concepts under realistic operating conditions, ASME GT2008-51191
- [4] Born, M., Wolf, E. (1964): Principles of optics, second edition, Pergamon Press Oxford, pp. 214
- [5] Boxx, I., Stöhr, M., Carter, C., Meier, W. (2009): Sustained multi-kHz flamefront and 3-component velocity-field measurements for the study of turbulent flames, *Appl. Phys. B* 95, pp. 23-29
- [6] Doll, U. Fischer, M., Stockhausen, G., Willert, C. (2012): Frequency scanning filtered Rayleigh scattering in combustion experiments, Lisbon, Portugal, 09-12 July
- [7] Fuyuto, T., Kronmayer, H., Lewerich, B., Bruebach, J., Fujikawa, T., Akihama, K., Dreier, T., Schulz, C. (2010): Temperature and species measurement in a quenching boundary layer on a flat-flame burner, *Exp. in Fluids* 49, pp. 783–795
- [8] Heinze, J., Meier, U., Behrendt, T., Willert, C., Geigle, K., Lammel, O., Lücknerath, R. (2011): PLIF thermometry based on measurements of absolute concentrations of the OH radical, *Z. Phys. Chem.* 225, pp. 1315-1341
- [9] Lefebvre, A. H. (1999): Gas turbine combustion, Taylor & Francis, ISBN 1-56032-673-5
- [10] Meier U, Heinze J, Freitag S, Hassa C (2011): Spray and flame structure of a generic injector at aeroengine conditions, GT2011-45282, Proceedings of ASME Turbo Expo, June 6-10, Vancouver, Canada
- [11] Morley, C. (2005): GASEQ - A chemical equilibrium program for windows;
<http://www.gaseq.co.uk/>
- [12] Sadanandan, R., Stoehr, M., Meier, W. (2008): Simultaneous OH-PLIF and PIV measurements in a gas turbine model combustor, *Appl. Phys. B*, 90, pp. 609-618
- [13] Singh, A., Mann, M., Kissel, T., Brübach, J., Dreizler, A. (2011): Simultaneous measurements of temperature and CO concentration in stagnation stabilized flames, *Flow Turbulence Combust.*, online DOI 10.1007/s10494-011-9384-6

- [14] Sweeney, M., Hochgreb, S. (2009): Autonomous extraction of optimal flame fronts in OH planar laser-induced fluorescence images, *Appl. Opt.* 48, 3866-3877
<http://www.opticsinfobase.org/ao/abstract.cfm?URI=ao-48-19-3866>
- [15] Trolier, R. (1988): Kinetic and spectroscopic studies of ozone photochemistry, Ph.D. Thesis, Cornell University
- [16] Voges, M., Klinner, J., Willert, C., Beversdorff, M., Schodl, R. (2007): Assessment of powder-based seeding materials for PIV applications in transonic, supersonic and reacting flows, 7th intern. Symp on PIV, Rome
- [17] Willert, C., Jarius, M. (2002): Planar flow field measurements in atmospheric and pressurized combustion chambers, *Experiments in Fluids* 33, pp. 931–939
- [18] Zhang, Rogg, B., Bray, K. (1996): Temporally and spatially resolved investigation of flame propagation and extinction in the vicinity of walls, *Combust. Sci. Tech.* 113, pp. 255-271